Model for hydrogen-atom production from the dissociation of fast H_n^+ cluster ions by thin foils

M. Farizon, N. V. de Castro Faria,* B. Farizon Mazuy, and M. J. Gaillard
Institut de Physique Nucléaire de Lyon, Institut National de Physique Nucléaire et de Physique des Particules–CNRS et Université Claude Bernard, 43, Boulevard du 11 Novembre 1918, 69622 Villeurbanne Cedex, France
(Received 31 October 1995; revised manuscript received 13 September 1996)

We present a quantitative model to describe the formation of hydrogen atoms ($1s$ and $2p$ states) following the dissociation of fast (30–120 keV/u) hydrogen cluster ions H_n^+ (n=2 and n= 3 – 21, odd) induced by a thin carbon foil. The model includes Coulomb explosion, multiple scattering, energy loss, and a simplified description of charge-exchange processes inside the solid. This description takes into account the dynamic screening of the moving protons by the target electrons and the relative position of the protons during the charge-exchange process. The results of the calculations performed with a Monte Carlo computer code reproduce remarkably well the experimental data. [S1050-2947(97)01301-2]

PACS number(s): 34.50.−s, 36.40+c

I. INTRODUCTION

When a fast hydrogen cluster goes through a thin solid target it is known that the relative populations of the $1s$ and $2p$ states of the hydrogen atoms produced are different from those obtained with isolated protons impinging on the same foil [1–3]. Indeed, just after traveling through the first atomic layers, the cluster has lost all its electrons. The protons of this ''crowd'' are repelled from each other by the screened Coulomb interaction. Protons that capture electrons inside or near the exit surface of the solid could occasionally leave the foil with an electron in the ground or excited states of the hydrogen atom, the probability of H^- formation being small. It was observed [1–3] that these capture and loss processes are influenced by the electronic screening of the protons in the solid and by the number and the position of neighboring protons during the interaction. This proximity effect is responsible for the differences between the cluster and the proton cases.

Recently [4], we have developed a Monte Carlo computer code to calculate the angular distribution of fragments of H_n^+ clusters after the traversal of a thin amorphous carbon foil. This code was based on models currently employed for fast molecular ions [5–7]. First, the incident cluster with a given structure was randomly orientated relative to the beam direction. This structure was obtained from *ab initio* calculations [8]. Second, Coulomb explosion, multiple scattering, and energy loss were introduced. Finally, the angular distribution at the exit surface was obtained.

In the present article, we have adapted this simulation code to take into account the possibility of one electron being lost or captured by a proton in the presence of its cluster partners in order to calculate the number of hydrogen atoms formed in the $1s$ and $2p$ states, and to compare these values to experimental data [1–3]. To do so, we have developed a simple model with a small number of free parameters that takes into account the main features of each phenomenon involved. In fact, we are dealing with a very complex situation and a first-principles approach would be, at present, quite difficult. Although simple, the model is able to reproduce the experimental results. It could be a good guide for a more complete description in the future.

II. MODEL

We first assume that the cluster fragments that emerge from the exit surface of the foil with bound electrons have picked them up at the target. Indeed, in all experiments we intended to describe [1–3], the target thickness was large enough to make sure that the transmission probability of the projectile with its own electrons was negligible [9,10]. Another assumption is related to the definition of electron-capture and loss cross sections for protons inside a solid. The existence of a stationary state of the projectile inside a solid depends on the collision rate and on the dynamic screening of the moving charge by the target electrons. This screening, also dependent on the particle velocity, results in the lowering of the binding energy with respect to the free-ion case and may prevent a quantum bound state in vacuum from being bound at all. It was suggested by Brandt [11] that the velocity dependence implies the existence of a velocity threshold below which a given state ceases to exist as a bound state. Recently, Müller and Burgdörfer [12] calculated this dynamical threshold for the He^+ case and obtained a value that is in impressive agreement with the one measured in our laboratory [13]. For protons, in the velocity range of interest here, the existence of the $1s$ state inside a carbon target was proposed theoretically by Cross [14] and experimentally demonstrated by Clouvas [15]. The existence of the $2p$ state inside the solid has been shown by Baudinet-Robinet and Dumont [16].

A. Isolated proton case

Our description begins with the comparison of the data available for the ratio of the electron-capture cross section (σ_c) over the electron-loss one (σ_1), measured with gaseous and solid carbon targets. This ratio is plotted in Fig. 1 as a function of the velocity v (a.u.) of the protons at the foil exit.

*Permanent address: Instituto de Fisica, Universidade Federal do Rio de Janeiro, Cx. postal 68528, Rio de Janeiro, RJ, 21945-970, Brazil.

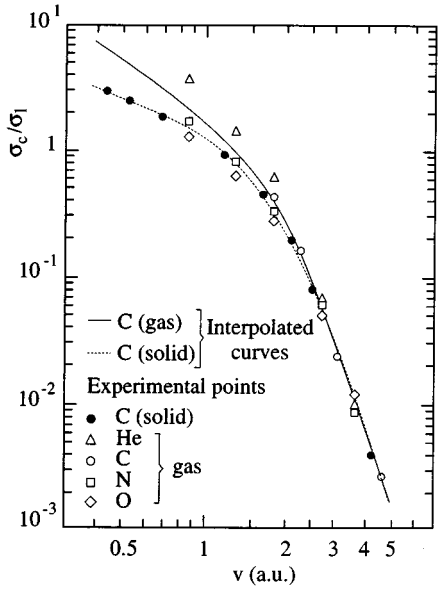

FIG. 1. The ratio of the electron-capture cross section (σ_c) to the electron-loss cross section (σ_1) for protons incident on different gaseous targets and on carbon foil, as a function of the proton velocity v. Experimental values and interpolated curves are shown.

The experimental values for the ''carbon gas'' target were extracted from gaseous carbon compounds [17] and an interpolation using He N, and O data was done for low velocities.

For the ''carbon-solid'' case, the data were extracted from the neutral fraction F_0, the number of neutral atoms emerging from the foil per incident proton. Assuming the existence of bound states in the solid F_0 is given at charge equilibrium, by

$$F_0=\frac{\sigma_{c\ \mathrm{solid}}}{\sigma_{1\ \mathrm{solid}}+\sigma_{c\ \mathrm{solid}}}, \tag{1}$$

where $\sigma_{c\ \mathrm{solid}}$ and $\sigma_{1\ \mathrm{solid}}$ are the capture and loss cross sections in a carbon solid target, respectively. From these data, for v greater than 2 a.u., the ratio σ_c/σ_1 measured with a gaseous target appears to be equal to the one measured with solid targets. Moreover, the data available for the electron-capture and loss cross sections (Fig. 2) show that

$$\sigma^{1s}_{c\ \mathrm{solid}}\approx\sigma^{1s}_{c\ \mathrm{gas}}$$

and

$$\sigma^{1s}_{1\ \mathrm{solid}}\approx\sigma^{1s}_{1\ \mathrm{gas}}. \tag{2}$$

In this velocity range, the solid target appears to be equivalent to a dense gas.

However, at lower velocities ($v\leqslant 2$ a.u.), we observe in Fig. 1 that the results obtained with solid targets are different from those corresponding to gaseous targets (for this velocity range, results with carbon gaseous targets were interpolated from the ones obtained with oxygen and nitrogen targets). The collision rate cannot be responsible for this fact because, even in the high velocity regime where the rate is important, gaseous and solid electron-loss cross sections are the same.

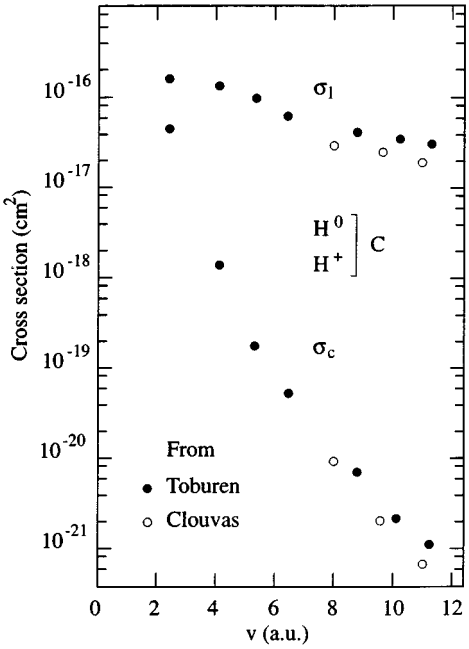

FIG. 2. The electron-capture and the electron-loss cross sections (σ_c and σ_1, respectively) for protons incident in gaseous (Toburen [17]) and solid (Clouvas [15]) carbon targets vs the proton velocity v.

Then we need to consider in that case the dynamic screening of the moving charge by the target electrons.

We assume that an electron bound to a swift proton in the solid is in an average potential well taken, for simplicity, as

$$V=-\frac{e^{-(r/a)}}{r}, \tag{3a}$$

where

$$a=\eta\frac{v}{v_0}+a_{\mathrm{TF}}. \tag{3b}$$

Here, a_{TF} is the Thomas-Fermi screening length, v_0 is the Bohr velocity, and η is a constant to be determined. In the high velocity regime ($v\rightarrow\infty$), $V\approx -1/r$, and for $v\rightarrow 0$, V is the static screened potential.

Rogers *et al.* [18] have calculated the electron energy levels of a hydrogenlike system with a potential well as the one we have defined. All the levels are shifted toward the continuum when the screening effect is increased. The main consequence of such a decrease of the binding energy is an increase of the loss cross section. To take into account the effect at low velocity of the free-electron gas on the loss cross section, we use a simplified formulation (corresponding to the Thomson classical expression) for the ratio between the loss cross sections for hydrogen atoms in the $1s$ state:

$$\frac{\sigma^{1s}_{1\ \mathrm{solid}}}{\sigma^{1s}_{1\ \mathrm{gas}}}=\frac{I^{1s}_0}{I^{1s}_{\mathrm{solid}}}, \tag{4}$$

where I_0^{1s} and I_{solid}^{1s} are the ionization energies of the free hydrogen atom and inside-solid hydrogen atom in the 1s state, respectively.

The electron capture is less influenced by the electron screening because the proton essentially captures localized electrons (conservation of energy and momentum). In other words, for capture occurring near a carbon nucleus, the delocalized electrons have little influence. For simplicity, we take

$$\sigma_{c\ \text{solid}}^{1s} = \sigma_{c\ \text{gas}}^{1s}. \tag{5}$$

In order to obtain the constant η of the expression (3b), we remember that almost all hydrogen atoms are produced in the ground state [3,19]. Consequently we can write

$$\frac{\sigma_{c\ \text{solid}}}{\sigma_{1\ \text{solid}}} = \frac{\sigma_{c\ \text{solid}}^{1s}}{\sigma_{1\ \text{solid}}^{1s}} \tag{6}$$

and we get

$$\frac{\sigma_{c\ \text{solid}}}{\sigma_{1\ \text{solid}}} = \frac{I_{\text{solid}}^{1s}}{I_0^{1s}} \frac{\sigma_{c\text{gas}}}{\sigma_{1\ \text{gas}}}. \tag{7}$$

With the known experimental ratio σ_c/σ_1 for gases and solids at different velocities, and using the ionization energies calculated by Rogers *et al.* [18], we can extract, by a least-square-fit procedure, the value of the constant η. The best fit corresponds to $\eta = 2.65$, with a deviation of less than 5%.

Concerning the production of atoms (per incident proton) in the $2p$ state, we use the same description as in the $1s$ case to define the fraction F_{2p}:

$$F_{2p} = \frac{\sigma_{c\ \text{solid}}^{2p}}{\sigma_{1\ \text{solid}}^{2p} + \sigma_{c\ \text{solid}}^{2p}}, \tag{8}$$

where $\sigma_{c\ \text{solid}}^{2p}$ and $\sigma_{1\ \text{solid}}^{2p}$ are the electron capture and loss cross sections for the 2p state in a carbon solid target, respectively. We have plotted in Fig. 3 the relative experimental values F_{2p} normalized at high velocity to F_0 versus v (a.u.). We introduce a normalization factor N because absolute values of the number of atoms in the $2p$ state are not available (to our knowledge). This normalization was possible because for v higher than 2 a.u., the velocity dependence of f_{2p} is the same as the F_0 one. However, this is not the case in the lower-velocity range.

The same kind of arguments presented in the case of the $1s$ state for electron capture and loss cross sections lead us to assume that, for electron loss,

$$\frac{\sigma_{1\ \text{solid}}^{2p}}{\sigma_{1\ \text{gas}}^{1s}} = \frac{I_0^{1s}}{I_{\text{solid}}^{2p}}, \tag{9}$$

where $\sigma_{1\ \text{solid}}^{2p}$ is the $2p$ state loss cross section in a carbon gas target. As stated previously, I_{solid}^{2p} is the ionization energy of the $2p$ state of the hydrogen atom in the target [18].

For the $2p$ level formation, we have considered only the direct electron capture, since the excitation from the $1s$ state (which results from an electron capture just at the exit of the foil) to the $2p$ state corresponds to a two-step collisional process. Indeed, the $2p$ capture cross section is of the order of one-eighth of the $1s$ capture cross section, but in the two-step process, the excitation following the electron capture has a small probability of occurring. Unfortunately, no experimental values are available in the literature for $\sigma_{c\text{gas}}^{2p}$, so that we take the approximation of Ref. [19]

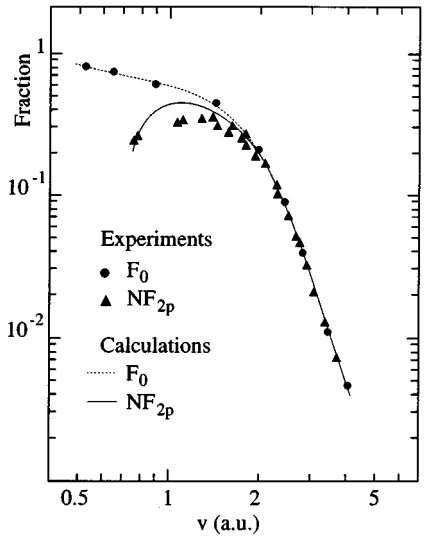

FIG. 3. Experimental values of the neutral fraction F_0, the number of neutral atoms emerging from the foil per incident proton and of the relative fraction NF_{2p}, the number of hydrogen atoms in the $2p$ state per incident proton normalized to F_0 (essentially $1s$ state) at high velocity. Calculated NF_{2p} and F_0 fractions (continuous curves) are also represented.

$$\sigma_{c\text{gas}}^{2p} = \frac{\sigma_{c\text{gas}}^{1s}}{2^3}. \tag{10}$$

The normalized fraction F_{2p} is calculated with the η value obtained from the neutral fraction data. In Fig. 3 are plotted the calculated F_{2p} and F_0 fractions. We get a fairly good agreement between our calculations and the experimental results. This agreement could probably be slightly improved by using a more sophisticated potential. In addition, since the experimental F_{2p} and F_0 fractions correspond to charge exchange in the last layers of the foil, the decrease of the electron-gas density in this region should be taken into account. However, the fact that our quite rough but simple description can reproduce the velocity dependence of the F_0 and F_{2p} fractions in the isolated proton case is a good indication that the main aspects of the electron loss or capture by a proton inside the solid have been taken into account.

B. Cluster case

In the case of H_n^+ clusters, each proton is inside the foil with $n-1$ neighbors. This proximity influences the charge-exchange processes, the main consequence being an increase of the ionization energy of the captured electron and a corresponding decrease of the loss cross section. From that point of view, we generalize the definitions of Sec. II A.

We first rewrite for the clusters the expression (4):

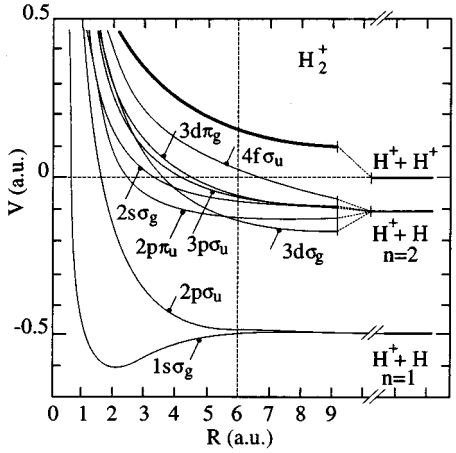

FIG. 4. Potential energy curves for the H_2^+ molecular ion leading to one H ($1s$ and $2p$ states) vs the proton distance R, adapted from Ref. [20]. The $V=0$ and the $R=6$ a.u. lines were drawn in order to clarify the explanation presented in Sec. II B.

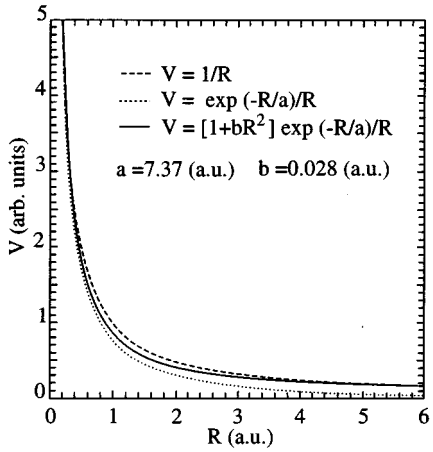

FIG. 5. Coulomb potentials with and without screening for two fixed values of a and b, vs the proton distance R. The screened potential with the correction term $(1+bR^2)$ (see text) is also represented.

$$\frac{\sigma^{1s,i}_{1\ \mathrm{solid}}}{\sigma^{1s}_{1\ \mathrm{gas}}}=\frac{I^{1s}_0}{I^{1s}_{i\ \mathrm{solid}}}, \tag{11}$$

where $I^{1s}_{1\ \mathrm{solid}}$, the ionization energy for an electron captured by a proton i surrounded by $n-1$ protons, depends on the relative distance between the protons.

Let us consider first the simple case of an isolated H_2^+. The ionization energy (difference between the energies of the two protons without and with one electron) can be written as the (positive) binding energy of the molecular state, $B^{1s}(R)$ [equal to - $V^{1s}(R)$ plotted in Fig. 4] plus the repulsion energy $(1/R)$ between the two protons:

$$I^{1s}(R)=B^{1s}(R)+\frac{1}{R}. \tag{12}$$

It is reasonable to assume that neutral atoms observed at the exit of the foil result from an electron capture just before emergence. If one proton moves close to a hydrogen atom in the $1s$ state, at a distance of the order of or greater than 6 a.u. (the most probable distance between two protons at the exit of the foil for the smallest clusters [4]), the energies of the molecular states (bonding or antibonding) do not change very much, as can be seen in Fig. 4. Consequently, the ionization energy is changed mainly by the quantity $1/R$.

We generalize this behavior in order to calculate the ionization energy in the case of one proton and one electron surrounded by $n-1$ protons inside the foil. We write the ionization energy of the ''$1s$ electron'' captured by a proton i surrounded by the crowd of $n-1$ other protons j as

$$I^{1s}_{i\ \mathrm{solid}}=B^{1s}_{i\ \mathrm{solid}}+\sum_{j=1,j\neq i}^{n}\left(\frac{e^{-(R_{i,j}/a)}}{R_{i,j}}(1+bR^2_{i,j})\right), \tag{13}$$

where $R_{i,j}$ represents the distance between the protons i and j. The first term represents the binding energy of the generalized molecular state for a system with n protons and one electron inside the solid, and the second one the screened repulsion energy between the protons. The term $B^{1s}_{i\ \mathrm{solid}}$, which depends on the distances between the protons, is not known even for H_2^+ inside the solid. By analogy with the free H_2^+ case, we assume that $B^{1s}_{i\ \mathrm{solid}}$ is constant and equal to the binding energy of one $1s$ electron captured by one proton inside the solid. For the screened repulsion energy we have introduced the factor $(1+bR^2_{i,j})$ in order to get more flexibility for our choice of the analytical form of the screening potential, particularly when the cluster velocity is small and the distance between the protons at the exit surface of the foil is large (see also Sec. III). In Fig. 5 the potential including the term $(1+bR^2)$ is drawn for a small value of the constant b. This term modifies essentially only the long-range part of the potential and consequently it has little influence on the lower hydrogen atomic states as calculated by Rogers *et al.* [18].

For the ''$2p$ state'' case, we write in a similar way for the electron-loss cross section

$$\frac{\sigma^{2p,i}_{1\ \mathrm{solid}}}{\sigma^{1s}_{1\ \mathrm{gas}}}=\frac{I^{1s}_0}{I^{2p}_{i\ \mathrm{solid}}}. \tag{14}$$

As before,

$$I^{2p}_{i\ \mathrm{solid}}=B^{2p}_{i\ \mathrm{solid}}+\sum_{j=1,j\neq i}^{n}\left(\frac{e^{-(R_{i,j}/a)}}{R_{i,j}}(1+bR^2_{i,j})\right). \tag{15}$$

The term for the repulsion energy is the same as in the $1s$ case. However, when we observe the potential-energy curves of H_2^+ corresponding to the $2p$ state (Fig. 4), we see that the states are mostly antibonding ones. To take approximately into account this average antibonding effect on the ionization energy, we assume the following expression:

$$B^{2p}_{i\ \mathrm{solid}}=I^{2p}_{\mathrm{solid}}+I^{i}_{ab}, \tag{16}$$

where

$$I^{i}_{ab}=\sum_{j=1,j\neq i}^{n}k(R_{i,j}-R_{\mathrm{cut}}) \quad \text{for } R_{i,j}\leqslant R_{\mathrm{cut}}$$

and

$$I^{i}_{\mathrm{ab}}=0 \quad \text{for } R_{i,j}>R_{\mathrm{cut}}.$$

The two free parameters k and R_{cut} have to be adjusted.

Concerning the electron capture, we notice that the L-shell electrons of carbon are roughly at 0.1 a.u. from the carbon nucleus. As the average distances between protons are very large compared to this, we neglect the proximity effect in the electron capture. Then, for the electron capture in the $1s$ state, we have

$$\sigma^{1s,i}_{c\ \mathrm{solid}}=\sigma_{c\ \mathrm{solid}}=\sigma^{1s}_{c\ \mathrm{gas}}. \tag{17}$$

For the electron capture cross-sections in the ''$2p$ state,'' using the same arguments as for the ''$1s$ state'' and expression (10), we write

$$\sigma^{2p,i}_{c\ \mathrm{solid}}=\sigma^{2p}_{c\ \mathrm{solid}}=\sigma^{2p}_{c\ \mathrm{gas}}=\frac{\sigma^{1s}_{c\ \mathrm{gas}}}{2^3}. \tag{18}$$

III. CALCULATIONS AND RESULTS

The Monte Carlo computer code has been described elsewhere [4]. In brief, the incident cluster has a configuration given by *ab initio* calculations [8], is randomly oriented, and is supposed to dissociate (losing all its electrons) in the front surface of the target. We describe the protons by classical orbits. The foil is divided into a large number of thin parallel slabs. From one slab to the next, the calculation of the proton trajectories takes into account the electronic energy loss, the influence of the superposed wake potentials, and the screened Coulomb explosion. This process is continued until the crowd of protons reaches the exit surface. Then the internuclear separations $R_{i,j}$ and the velocities (absolute values and directions) are registered and their values stored.

As already explained, the decisive charge exchange involved in neutral atom production takes place in the last layers of the foil, near the exit surface. Consequently we do not include, even in the $1s$ case, the possibility of charge exchange for each slab and we introduce the possibility of charge exchange only when the $R_{i,j}$ distances and the velocities have been obtained for each cluster at the exit surface of the foil. We suppose that the charge equilibrium is attained and we associate with each proton of one cluster a probability of leaving the foil with one electron ($1s$ or $2p$), with cross sections calculated as stated in Sec. II. The choice is made by generating pseudorandom numbers that have the same probability distribution as the event. We begin the analysis with the proton that has the smallest ionization energy. All the protons of the cluster get a chance to capture an electron. To take into account the effect of an electron bound on one proton of the cluster, we substract the contribution of this proton to the loss cross sections of the others.

The results of our calculations are presented in Figs. 6, 7, and 8. The first two show the experimental neutral fractions [1,2] and the results of the calculations for clusters H_n^+ ($n=2$ and $n=1$–21, odd) with energies of 30, 40, 60, 80, and 120 keV/u incident on a carbon target of 2.1 μg/cm^2 (Fig. 6) and 3.4 μg/cm^2 (Fig. 7). The agreement is, in general, excellent if we remember that only the parameter b [velocity dependent, see expression (15)] was left free in our $1s$ calculations, the parameter η being fixed with the value 2.65 as explained in Sec. II A.

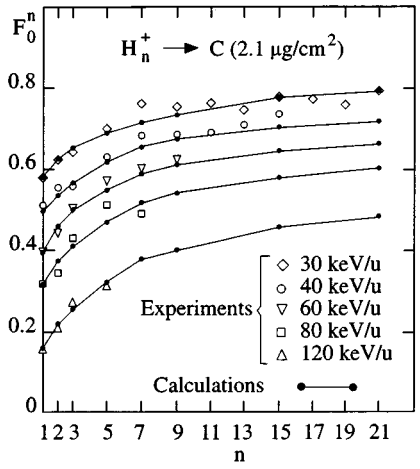

FIG. 6. Experimental [1,2] and calculated neutral fractions ($1s$ state) vs the cluster mass number n ($n=2$ and $n=1$–21, odd) for energies of 30, 40, 60, 80, and 120 keV/u incident on a carbon target of 2.1 μg/cm^2.

Table I presents the values of the b parameter for the various velocities. Calculations have also been done with $b=0$, the proximity effect being then underestimated. Indeed, with $b=0$ the calculated F_0 fraction is found to be smaller (25%) than the experimental value (cluster case) at the lowest energies. The difference between the experimental and calculated values decreases with increasing velocity. Since in the isolated proton case the velocity dependence has been tested previously, and since the distance between the protons at the exit of the foil decreases with increasing velocity, we have introduced the correction term $(1+bR^2_{i,j})$ for large distances between the protons at the exit of the foil, i.e.,

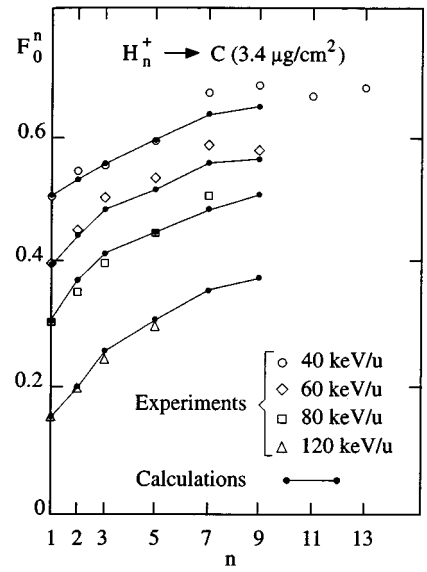

FIG. 7. Experimental [1,2] and calculated neutral fractions ($1s$ state) vs the cluster mass number n ($n=2$ and $n=1$–21, odd) for energies of 40, 60, 80, and 120 keV/u incident on a carbon target of 3.4 μg/cm^2.

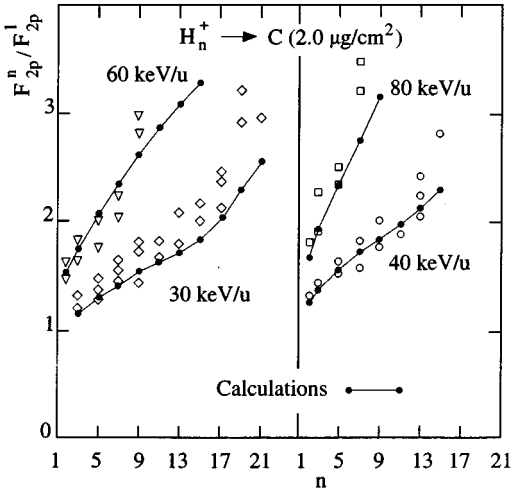

FIG. 8. Experimental [3] and calculated neutral fractions F_{2p}^n normalized to the proton fractions F_{2p}^1 vs the cluster mass number n ($n=2$ and $n=1-21$, odd) for energies of 30, 40, 60, and 80 keV/u incident on a carbon target of 2.0 μg/cm^2.

approximately 5–15 a.u. We assume that the velocity dependence of the energy of the atomic states is not modified by this long-range correction.

Figure 8 presents, for clusters of various sizes and energies impinging on a 2.0 μg/cm^2 carbon target, the fraction F_{2p}^n normalized to the proton fraction F_{2p}^1. For the $2p$ case, we use the same values of the parameter b but we still have two free parameters k and $R_{\rm cut}$, the values of which (0.055 and 15.1 a.u., respectively) were extracted from the data at one velocity. The calculations are in good agreement with the experimental results. The variation of the F_{2p}^n fraction with the cluster size, different from the F_{1s} one, is well reproduced at all velocities.

IV. DISCUSSION AND CONCLUSIONS

The excellent agreement between calculations and experimental results presented in Figs. 6 and 7 does not seem to be fortuitous. It is remarkable that we reproduce well, in the $1s$ case, absolute neutral fractions for different velocities, clusters, and target thicknesses with only one free velocity-dependent parameter b. Table I shows that the values of this parameter are small and coherent for the different velocities. It is clear that the main aspects of the charge-exchange processes are well described by our simplified model.

TABLE I. Values of the parameters a and b (free) of the screened potential $V=[\exp(-R_{i,j}/a)/R_{i,j}]\ (1+bR_{i,j}^2)$, where $a=2.65v/v_0+a_{\rm TF}$, used in the calculations for different velocities. The free parameters of the model (k and $R_{\rm cut}$) intoduced for the $2p$ case have the following values: $k=0.055$ a.u. and $R_{\rm cut}=15.1$ a.u. for all velocities.

keV/u	a (a.u.)	b (a.u.)
30	6.62	0.042
40	7.41	0.028
60	8.83	0.022
80	10.11	0.020

Although the capture and loss of a $2p$ electron is a very complex problem, we have simulated in our work the $2p$ fraction yield with the same screening potential used in the $1s$ case. This oversimplification can be responsible for some deformations. The $2p$ fraction appears to be very sensitive to the screening effects in the 2–15 a.u. range. This is observed from the velocity dependence in the isolated proton case and from the proximity effects in the H_n^+ cluster case. Therefore, the F_{2p} fraction is an interesting tool to test the screening effect. More data, especially with different solid targets in order to change the electron density, should enable a more accurate description.

Finally, we have shown that the enhanced neutralization of a proton belonging to a hydrogen cluster ion H_n^+ ($n=2$ and $n=3-21$, odd) with velocity near the Bohr velocity was quantitatively reproduced using a simple model of the charge-exchange processes inside the foil. The model describes well the neutralization or population of the $1s$ and $2p$ states, showing that the charge exchanges including the screening and the proximity effect were the fundamental phenomena of the observed enhancement in spite of the difference observed in the cluster size dependence of the F_0 and F_{2p} fractions.

ACKNOWLEDGMENTS

One of the authors (N.V.C.F.) gratefully acknowledges the hospitality received from researchers and staff members of the Institut de Physique Nucléaire (IPN-Lyon) during his stay in France, and the support of the Conselho Nacional de Desenvolvimento Científica e Tecnológico.

[1] B. Mazuy, A. Belkacem, M. Chevallier, M. J. Gaillard, J. C. Poizat, and J. Remillieux, Nucl. Instrum. Methods B **28**, 497 (1987).

[2] B. Mazuy, J. Désesquelles, A. Belkacem, M. Chevallier, M. J. Gaillard, J. C. Poizat, and J. Remillieux, Nucl. Instrum. Methods B **33**, 105 (1988).

[3] M. Farizon, A. Clouvas, N. V. de Castro Faria, B. Farizon-Mazuy, M. J. Gaillard, E. Gerlic, A. Denis, J. Désesquelles, and Y. Ouerdane, Phys. Rev. A **43**, 121 (1991).

[4] M. Farizon, N. V. de Castro Faria, B. Farizon-Mazuy, and M. J. Gaillard, Phys. Rev. A **45**, 179 (1992).

[5] R. Schectman and W. D. Ruden, Nucl. Instrum. Methods **194**, 295 (1982).

[6] J. Kemmler, P. Koschar, M. Burkhard, and K. O. Groeneveld, Nucl. Instrum. Methods B **12**, 62 (1985).

[7] C. Deutsch, Phys. Rev. E **51**, 619 (1995).

[8] M. Farizon, B. Farizon-Mazuy, N. V. de Castro Faria, and H. Chermette, Chem. Phys. Lett. **177**, 451 (1991); M. Farizon, B. Farizon-Mazuy, and H. Chermette, J. Chem. Phys. **96**, 1325 (1992).

[9] M. J. Gaillard, J. C. Poizat, A. Ratkowski, J. Remillieux, and M. Auzas, Phys. Rev. A **6**, 2323 (1977).
[10] N. Cue, N. V. de Castro Faria, M. J. Gaillard, J. C. Poizat, and J. Remillieux, Nucl. Instrum. Methods **170**, 67 (1980).
[11] W. Brandt, *Atomic Collisions in Solids*, edited by S. Datz *et al.* (Plenum, New York, 1973), p. 261.
[12] J. Müller and J. Burgdörfer, Phys. Rev. A **43**, 6027 (1991).
[13] M. Chevallier, A. Clouvas, N. V. de Castro Faria, B. Farizon-Mazuy, M. J. Gaillard, J. C. Poizat, and J. Remillieux, Phys. Rev. A **41**, 1738 (1990).
[14] M. C. Cross, Phys. Rev. B **15**, 602 (1977).
[15] A. Clouvas, Doct. ès-Sciences, thesis, Université Lyon I, 1985.
[16] Y. Baudinet-Robinet and P. D. Dumont, Phys. Rev. A **29**, 1825 (1982).
[17] L. H. Toburen, M. Y. Nakai, and R. A. Langley, Phys. Rev. **171**, 114 (1968).
[18] F. J. Rogers, H. C. Craboske, Jr, and D. J. Harwood, Phys. Rev. A **1**, 1537 (1970).
[19] J. R. Oppenheimer, Phys. Rev. **31**, 349 (1928).
[20] T. E. Sharp, At. Data **2**, 119 (1971).